

CO₂ ReductionReduction of CO₂ by Pyridine Monoimine Molybdenum Carbonyl Complexes: Cooperative Metal–Ligand Binding of CO₂Daniel Sieh,^[a] David C. Lacy,^[a] Jonas C. Peters,^[a] and Clifford P. Kubiak^{*[a, b]}

Abstract: [(^{Ar}PMI)Mo(CO)₄] complexes (PMI = pyridine monoimine; Ar = Ph, 2,6-di-*iso*-propylphenyl) were synthesized and their electrochemical properties were probed with cyclic voltammetry and infrared spectroelectrochemistry (IR-SEC). The complexes undergo a reduction at more positive potentials than the related [(bipyridine)Mo(CO)₄] complex, which is ligand based according to IR-SEC and DFT data. To probe the reaction product in more detail, stoichiometric chemical reduction and subsequent treatment with CO₂ resulted

in the formation of a new product that is assigned as a ligand-bound carboxylate, [(^{Pr₂Ph}PMI)Mo(CO)₃(CO₂)]²⁻, by NMR spectroscopic methods. The CO₂ adduct [(^{Pr₂Ph}PMI)Mo(CO)₃(CO₂)]²⁻ could not be isolated and fully characterized. However, the C–C coupling between the CO₂ molecule and the PDI ligand was confirmed by X-ray crystallographic characterization of one of the decomposition products of [(^{Pr₂Ph}PMI)Mo(CO)₃(CO₂)]²⁻.

Introduction

Rising levels of atmospheric carbon dioxide threaten global climate change and thus efforts towards renewable solar energy have stimulated interest in the electrochemical conversion of CO₂ into a solar fuel. The selective reduction of carbon dioxide to a specific fuel product is currently not possible with heterogeneous electrocatalysts whereas molecular catalysts can, in principle, afford high selectivity. However, the potentials at which CO₂ is reduced with molecular catalysts are usually more negative than –1.8 V vs. [Cp₂Fe] in acetonitrile and they rarely operate in aqueous media. Therefore, efforts to lower the overpotential at which CO₂ is reduced represent a challenge in molecular electrocatalysis.^[1] Another advantage of using molecular catalysts is the tunability that is intrinsically available when working with organic/organometallic ligands. Informed choices in new ligands and/or ligand modifications may provide the means to lower the overpotential required to achieve catalysis at high current densities.

A current hypothesis in molecular based CO₂-reduction electrocatalysis is the necessity for so-called ligand redox non-innocence, whereby the ligand accepts one or more electrons from

a metal center or an electrode. For example, the [(bipyridine)-Re(CO)₃]^[2,3] system has been thoroughly characterized^[4–6] and significant evidence supports the notion that the reduced compound that binds CO₂ is a [(bipy)Re⁰(CO)₃]⁻ complex. The redox potential of the metal ion is somewhat fixed within a given ligand framework. However, by tuning the ligand one can change the potentials at which CO₂ is reduced. This has been accomplished previously by modifying the substituents on the bipy ligand.^[6,7]

Recently, we and others reported the electrochemical reduction of CO₂ with the related [(bipy)Mo(CO)₄]^[8] complex and found evidence for electrocatalysis with a formally 18-electron [(bipy)Mo(CO)₃]²⁻ complex by reduction of a 19-electron [(bipy)Mo(CO)₄]⁻ at –2.68 V vs. [Cp₂Fe].^[9,10] This reduction process is likely ligand based and consequently it was rationalized that by switching to an iminopyridine ligand, a more positive reduction potential would result. This hypothesis is supported by a previous report which directly compared the electronic properties of [(bipy)Re^I(CO)₃Cl] and [(^{Ph}PMA)Re^I(CO)₃Cl] (PMA = pyridine monoaldimine) demonstrating that by exchanging a pyridine moiety for an imine group with an aryl substituent the redox potential of the ligand shifts positively by approximately 400 mV.^[11] Moreover, there is precedent of pyridine diimine (PDI)-supported cobalt-based molecular electrocatalysis for CO₂ reduction^[12] and it seemed likely that this could be extended to other metal ions. Herein we report our findings using pyridine monoimine (PMI) molybdenum tetracarbonyl precursors (Figure 1) towards electrochemical and stoichiometric CO₂ reduction and show evidence that the fully reduced Mo complex binds the CO₂ carbon atom on the ligand and the oxygen atom on the metal center.

[a] Dr. D. Sieh,⁺ Dr. D. C. Lacy,⁺ Prof. Dr. J. C. Peters, Prof. Dr. C. P. Kubiak
Joint Center for Artificial Photosynthesis
Division of Chemistry and Chemical Engineering
California Institute of Technology
1200 East California Boulevard, Pasadena, CA 91125 (USA)
E-mail: ckubiak@ucsd.edu

[b] Prof. Dr. C. P. Kubiak
Department of Chemistry and Biochemistry
University of California, San Diego
9500 Gilman Drive MC 0358, La Jolla, California 92093 (USA)

[⁺] These authors contributed equally to this work.

Supporting information for this article is available on the WWW under <http://dx.doi.org/10.1002/chem.201500463>.

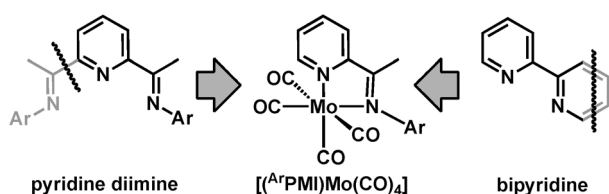


Figure 1. Inspiration for utilization of the pyridine monoimine ligands (A PMI, Ar = Ph, 2,6-diisopropylphenyl) derived from CO₂ reduction catalysts, which used bipyridine and pyridine diimine moieties.

Results and Discussion

Syntheses and characterization

The phenyl and diisopropyl derivatives of the pyridine monoimine ligands, Ph PMI and iPr_2Ph PMI, respectively, were synthesized by condensation reactions with 2-acetylpyridine and the appropriate aniline under azeotropic removal of water in toluene. The complexes $[(^{iPr_2Ph}PMI)Mo(CO)_4]$ and $[(^{Ph}PMI)Mo(CO)_4]$ were synthesized by heating the appropriate ligand with Mo(CO)₆ at reflux in toluene. After removal of the solvent, washing of the residue with pentane, and recrystallization, the complexes $[(^{iPr_2Ph}PMI)Mo(CO)_4]$ and $[(^{Ph}PMI)Mo(CO)_4]$ were obtained in 64% and 69% yield, respectively, as analytically pure solids. ¹H and ¹³C NMR spectroscopic characterization of the complexes is consistent with the respective PMI ligand framework and three carbonyl resonances can be detected in the ¹³C NMR spectra, indicating two equivalent axial and two additional unique carbonyl ligands *trans* to the PMI ligand and an overall C_s symmetry. To compare the electronic properties of the PMI ligands to the parent bipy ligand, the CO stretching frequencies were probed by FTIR spectroscopy (Table 1).

| Ligand | bipy ^[9] | Ph PMI | iPr_2Ph PMI |
|--------------------------------|---------------------|-------------|------------------|
| ν(CO) | 2016 | 2014 | 2011 |
| | 1904 | 1904 | 1899 |
| | 1877 | 1885 | 1883 |
| | 1832 | 1837 | 1839 |
| E _{1/2} | -1.98 | -1.80 | -1.81 |
| E _{cp} ^[b] | -2.54 | -2.35 | -2.55 |

[a] CH₃CN solution; [b] peak potential of the irreversible 2nd reduction at 100 mV s⁻¹.

No significant differences were detected in the C≡O stretching vibrations of the three complexes, indicating similar electronic properties.

Single crystals suitable for X-ray diffraction experiments could be obtained for $[(^{Ph}PMI)Mo(CO)_4]$ and $[(^{iPr_2Ph}PMI)Mo(CO)_4]$. The ORTEP representation of the molecular structure of $[(^{iPr_2Ph}PMI)Mo(CO)_4]$ and selected bonding parameters are given in Figure 2. Both complexes exhibit a distorted octahedral geometry, indicated by a bond angle < 180° between the axial

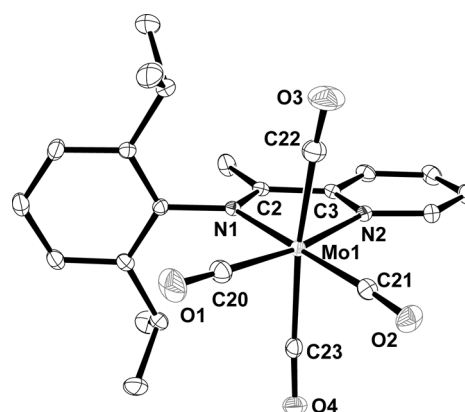


Figure 2. ORTEP representation of the molecular structure of $[(^{iPr_2Ph}PMI)Mo(CO)_4]$ with ellipsoids shown at the 50% probability level. Hydrogen atoms are omitted for clarity. Selected bond lengths (Å) and angles (°) for one of the two independent molecules in the asymmetric unit: Mo1–N1 2.2453(13), Mo1–N2 2.2465(12), Mo1–C20 1.9702(16), Mo1–C21 1.9568(16), Mo1–C22 2.0621(19), Mo1–C23 2.0326(17), C20–O1 1.1561(19), C21–O2 1.167(2), C22–O3 1.140(2), C23–O4 1.153(2), N1–C2 1.2965(18), C2–C3 1.478(2); N1–Mo1–C21 173.89(6), N2–Mo1–C20 169.45(6), N1–Mo1–N2 71.69(5), N2–Mo1–C21 103.11(6), N1–Mo1–C20 98.01(6), C20–Mo1–C21 87.30(7), C22–Mo1–C23 168.41(7), Mo1–C20–O1 179.35(18), Mo1–C21–O2 176.26(15), Mo1–C22–O3 173.64(17), Mo1–C23–O4 171.33(14).

carbonyl carbon atoms and the Mo metal center (C22–Mo1–C23: 165–168°). There are no significant differences between the C–O bond lengths within the two PMI complexes and $[(bipy)Mo(CO)_4]$.^[13] The CO ligands *trans* to N_{py} in the PMI complexes have shorter C–O bond lengths than those in $[(bipy)Mo(CO)_4]$ (ca. 1.156 Å compared ca. 1.164 Å) indicating that the PMI ligands are stronger π-acids. However, the difference of approximately 0.01 Å is too small to make a conclusive statement. For related pyridine diimine ligands, elongation of the imine double bonds and shortening of the exocyclic C–C bonds have been used to quantify the amount of electron transfer to the ligand.^[14] Comparing these bond lengths of $[(^{iPr_2Ph}PMI)Mo(CO)_4]$ with the bond lengths observed for those of the free ligand,^[15] only small changes were found (N1–C2: $^{iPr_2Ph}PMI$: 1.2801(17), $[(^{iPr_2Ph}PMI)Mo(CO)_4]$: 1.2965(18); C2–C3: $^{iPr_2Ph}PMI$: 1.4959(18), $[(^{iPr_2Ph}PMI)Mo(CO)_4]$: 1.478(2)), indicating that the ligand is essentially neutral in the octahedral Mo tetracarbonyl complexes.

Electrochemistry

The electrochemical properties of the PMI complexes were investigated by cyclic voltammetry (CV) in MeCN (Figure 3). Each complex exhibits a reversible one-electron process assigned to the $[(^A)PMI)Mo(CO)_4]/[(^A)PMI)Mo(CO)_4]^-$ redox couple. We propose that $[(^A)PMI)Mo(CO)_4]^-$ is best described as having a ligand anion radical similar, to previously studied bipy^[3,5] and PD^[5,16] platforms. This assignment is also favored in light of infrared-spectroelectrochemical (IR-SEC) results (see below) and the E_{1/2} values (Table 1) are further evidence for a ligand-based reduction in that the process occurs at approximately 200 mV more positive than $[(bipy)Mo(CO)_4]$. A second irreversible reduction process occurs at -2.35 V for $[(^{Ph}PMI)Mo(CO)_4]$ and

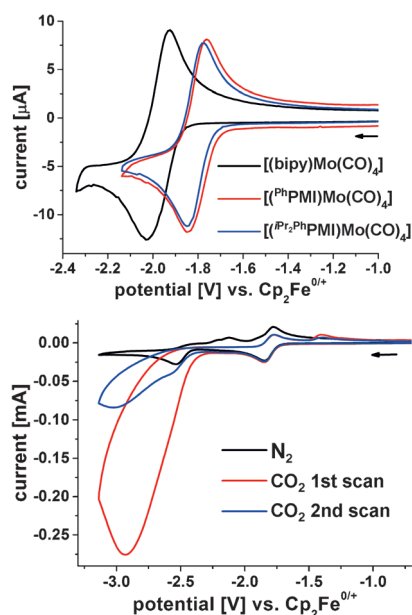


Figure 3. Cyclic voltammograms of $[(\text{Pr}_2\text{PhPMI})\text{Mo}(\text{CO})_4]$ in MeCN in the presence and absence of CO_2 (bottom, 200 mV s^{-1}) and a comparison of the isolated reversible reduction for $[(\text{bipy})\text{Mo}(\text{CO})_4]$, $[(\text{Pr}_2\text{PhPMI})\text{Mo}(\text{CO})_4]$, and $[(\text{PhPMI})\text{Mo}(\text{CO})_4]$ (top, 100 mV s^{-1}). Conditions: $0.1 \text{ M } [n\text{Bu}_4\text{N}]\text{PF}_6$; working electrode = glassy carbon; auxiliary electrode = carbon rod; reference electrode = Ag/AgNO_3 (1 mm) in an isolated chamber with $0.1 \text{ M } [n\text{Bu}_4\text{N}]\text{PF}_6$ separated with a Vycor tip.

-2.55 V for $[(\text{Pr}_2\text{PhPMI})\text{Mo}(\text{CO})_4]$ and this is assigned to forming the fully reduced species $[(\text{ArPMI})\text{Mo}(\text{CO})_3]^{2-}$. The loss of a CO ligand would be consistent with the irreversibility of the CV wave of the second reduction and is further supported by IR and ^{13}C NMR spectroscopy (see below) for the chemically reduced complex $[(\text{Pr}_2\text{PhPMI})\text{Mo}(\text{CO})_4]$. Since the shape of the first redox couple does not significantly change in MeCN, even after passing the potential for the second reduction (see the Supporting Information, Figure S16), we cannot make a definite statement about the loss of the CO ligand on the CV time-scale.

In CO_2 -saturated MeCN solution under an atmosphere of CO_2 , a current enhancement is observed for $[(\text{Pr}_2\text{PhPMI})\text{Mo}(\text{CO})_4]$ to take place with an onset at approximately -2.4 V and peaks at -2.9 V indicative of catalytic behavior. However, repeating the scan diminished the current enhancement, which could not be recovered by stirring the solution or by introducing more CO_2 . Electrochemistry in CO_2 -saturated THF did not exhibit significant catalytic current enhancement within the limits of the solvent window for CO_2 -saturated THF (see the Supporting Information, Figure S21). A one-hour bulk electrolysis measurement in MeCN at -2.5 V vs. the Ag/AgNO_3 reference electrode resulted in formation of CO, but only in 10% Faradaic efficiency (we note that only trace H_2 was formed during this process). The CO generated during bulk electrolysis is likely due to the formation of $[(\text{ArPMI})\text{Mo}(\text{CO})_3]^{2-}$.

To understand the nature of these electron transfers, we investigated the complex $[(\text{Pr}_2\text{PhPMI})\text{Mo}(\text{CO})_4]$ with infrared-spectroelectrochemical methods^[17] (Figure 4).

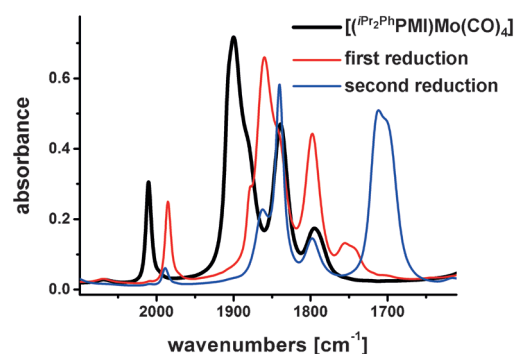


Figure 4. $\text{C}\equiv\text{O}$ region of the IR spectra derived from the IR-SEC experiment. Conditions: $0.1 \text{ M } [n\text{Bu}_4\text{N}]\text{PF}_6$ in MeCN; working electrode = Ag; auxiliary electrode = Pt; pseudo reference electrode = Ag.

At open circuit potential, the IR spectrum of the neutral complex is reproduced in the IR-SEC cell. Upon stepping the potential into the first reduction, all four carbonyl stretching vibrations are shifted towards lower frequencies and now occur at $1985, 1860, 1843,$ and 1798 cm^{-1} , indicating stronger back bonding to the carbonyls. The small shift of about $30\text{--}40 \text{ cm}^{-1}$ however indicates that the reduction is mostly localized at the PMI ligand. At potentials of the second reduction a more drastic change can be observed. Three carbonyl stretching vibrations can now be detected at $1840, 1712$ and 1701 cm^{-1} , indicating significantly stronger back bonding. The results of the IR-SEC experiment are in good agreement with the IR data for neutral, mono- and doubly-reduced tungsten carbonyl bipyridine complexes obtained by chemical reduction.^[9]

Chemical reduction and reaction with CO_2

To gain insight into the electrochemical behavior of the PMI-Mo complexes in presence of CO_2 , we investigated the chemical reduction and subsequent reaction with CO_2 . Reduction of the complex $[(\text{Pr}_2\text{PhPMI})\text{Mo}(\text{CO})_4]$ was achieved using an excess of KC_8 in $[\text{D}_8]\text{THF}$, which led to a quick color change from red to orange^[18] to violet. Attempts to crystallize the rather sensitive orange and/or violet species have been unsuccessful. However, the ^1H and ^{13}C NMR spectra of the violet species suggest the clean formation of a single product that is formulated as $[(\text{Pr}_2\text{PhPMI})\text{Mo}(\text{CO})_3]^{2-}$. ^1H NMR spectroscopic investigation of the violet product after filtration from graphite revealed a remarkable upfield shift of the resonances of the pyridine protons, which is also evident in some of the ^{13}C NMR resonances. The largest shift can be observed in the imine carbon resonance, which is detected at $\delta = 172 \text{ ppm}$ in the neutral compound and is shifted to 118 ppm in the doubly reduced form. A correlation of upfield shifts of ^{13}C NMR resonances upon electron transfer to the ligand backbone has been previously discussed for PDI complexes.^[19] Only one carbonyl resonance can be observed in the ^{13}C NMR spectrum, at $\delta = 245 \text{ ppm}$, which is consistent with the loss of one carbonyl ligand and fast exchange of the remaining three ligands on the NMR time-scale at room temperature.^[20] Furthermore, the carbonyl resonance is shifted to higher frequencies compared to the neutral

parent complex, consistent with stronger back bonding to the carbonyl ligands.^[21] The loss of one CO ligand is also supported by headspace analysis (GC) of one of the reactions, which showed the formation of CO in the order of magnitude of the reaction size. FTIR spectra of freshly prepared solutions of $[(^{iPr_2Ph}PMI)Mo(CO)_3]^{2-}$ in THF or $[D_8]THF$ provided carbonyl stretching vibrations at 1845, 1719, and 1700 cm^{-1} . These frequencies are nearly identical to those observed in the IR-SEC for the doubly reduced species. To further corroborate these stretching frequencies with the IR-SEC data, the chemical reduction was performed in $[D_3]MeCN$. Although the NMR spectrum is not as clean as those obtained in $[D_8]THF$ (as expected for KC_8 reduction in MeCN), similar upfield shifts in the 1H NMR spectrum were observed. Additionally, freshly prepared THF solutions $[(^{iPr_2Ph}PMI)Mo(CO)_3]^{2-}$ could be stripped of solvent and dissolved in MeCN, from which the main features (1840, 1712 and 1701 cm^{-1}) of the IR spectrum obtained by electrochemical reduction were reproduced (see the Supporting Information, Figure S27).

Reaction of the in situ-prepared violet, doubly reduced complex $[(^{iPr_2Ph}PMI)Mo(CO)_3]^{2-}$ with CO_2 led to a color change to pale yellow/brown and 1H NMR spectroscopic investigation of the reaction products revealed the formation of a major product alongside small amounts of unidentified side products. Using $[Cp^*Fe]$ as an internal standard, an NMR yield of 80(10)% could be established, indicating that the majority of the dianion $[(^{iPr_2Ph}PMI)Mo(CO)_3]^{2-}$ is converted into this major product. The detection of two resonances for the methine protons, as well as the protons in the 3 and 5 positions and 4 resonances for the isopropyl methyl groups, suggests the loss of the mirror plane, which is present in the neutral and reduced parent complexes. The 1H and ^{13}C NMR resonances show significant broadening, which might be attributed to a fluxional process, that is, K^+ coordination/decoordination. This view is supported by a significant sharpening of

the resonances upon addition of 18-crown-6 or recording the NMR spectra in $[D_7]DMF$ of a sample that was originally prepared in THF. A ^{13}C NMR resonance for the CO ligands can be estimated at $\delta=236$ ppm as a very broad signal (in $[D_8]THF$ and $[D_7]DMF$) suggesting that the exchange of the three CO ligands is slow compared to the parent compound. Two ^{13}C NMR resonances are observed at $\delta=185$ and 173 ppm in the region expected for imine-carbon and pyridine carbon atoms typical for PDI-metal complexes (Figure 5), both of which show coupling to the protons of the methyl group of the parent imine moiety ($\delta=1.14$ ppm, $N-CCH_3$) in the $^1H,^{13}C$

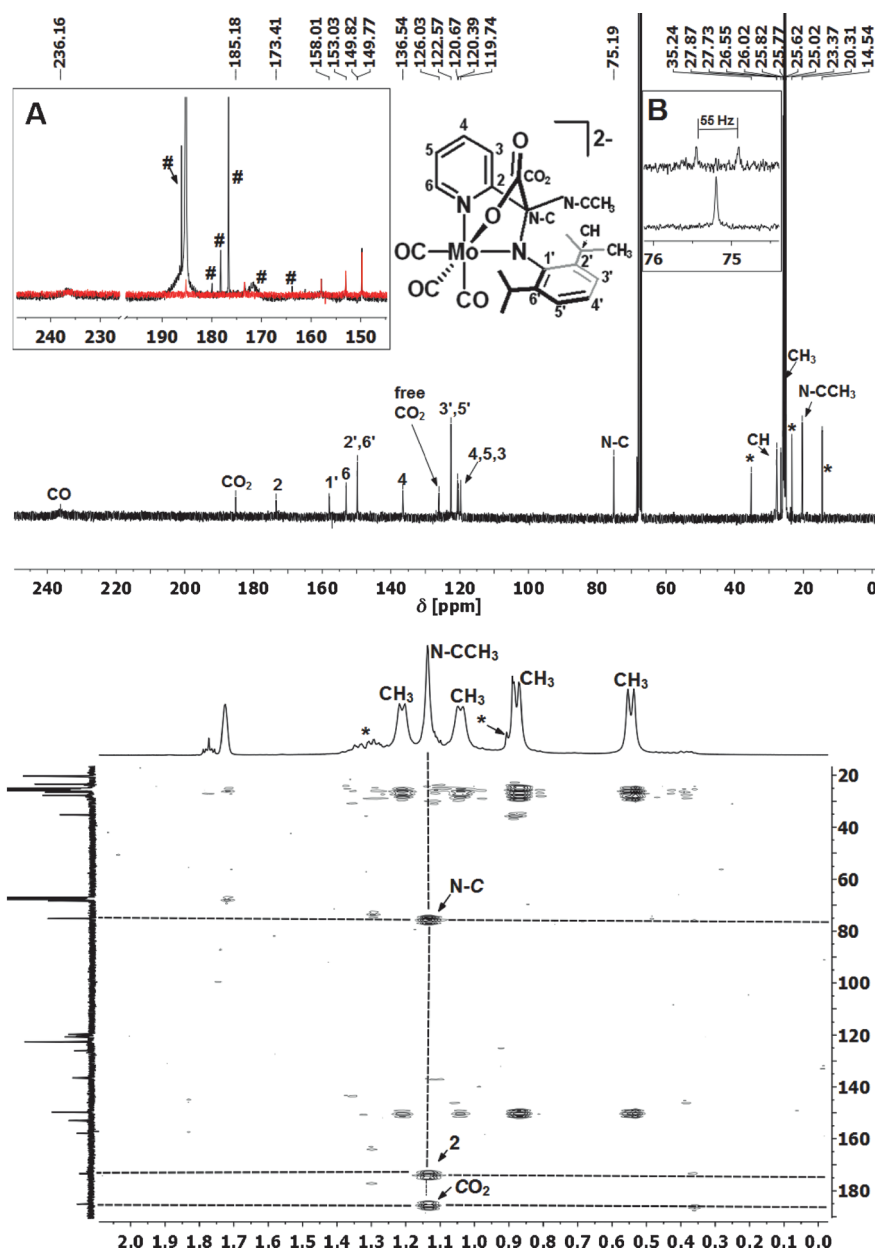
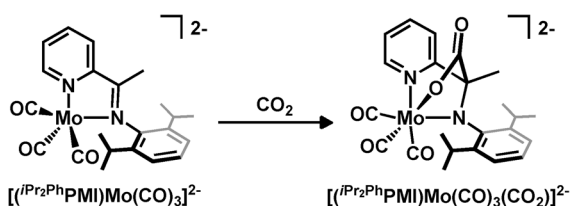


Figure 5. NMR spectroscopic characterization of the product of the reaction of $[(^{iPr_2Ph}PMI)Mo(CO)_3]^{2-}$ with CO_2 in $[D_8]THF$. Top: Portion of the $^1H,^{13}C$ HMBC NMR spectrum. Bottom: ^{13}C NMR spectrum including labeling scheme. Inset A: Strong enhancement of the resonance at 185 ppm in the reaction with $^{13}CO_2$ (black) compared to the reaction with non-enriched CO_2 (red). Spectra are normalized to the resonance at 20.3 ppm. Inset B: Splitting of the resonance at 75 ppm in the reaction with $^{13}CO_2$. *: pentane; #: $^{13}CO_2$ incorporation in side/decomposition products.

HMBC NMR spectrum. The resonance at $\delta = 185$ ppm is strongly enhanced when $^{13}\text{CO}_2$ is used (Figure 5, inset A), suggesting incorporation of the CO_2 carbon atom. Moreover, it indicates that the resonance at $\delta = 185$ ppm is not a PMI ligand resonance. Interestingly, the $^1\text{H},^{13}\text{C}$ HMBC NMR spectrum revealed that the methyl protons are also coupled to a ^{13}C NMR resonance at $\delta = 75$ ppm, which is an uncommon shift for a PMI ligand.

This ^{13}C NMR resonance is split into a doublet with a coupling constant of 55 Hz in the ^{13}C labeled compound (Figure 5, inset B), which is consistent with coupling to the carbon atom in $^{13}\text{CO}_2$ and is in the range of $^1J_{\text{C-C}}$ coupling constants for substituted carbonic acid/ester ($\text{RO}(\text{O}=\text{C})\text{R}'$).^[22] Furthermore the ^1H NMR resonance at $\delta = 1.14$ ppm is split into a doublet with a coupling constant of 3 Hz in the labeled complex (see the Supporting Information, Figure S29), which is not uncommon for a 3-bond C,H coupling.^[22]

Taken together, the findings from the NMR spectroscopic investigation of the product obtained by treating $[(^i\text{Pr}_2\text{PhPMI})\text{Mo}(\text{CO})_3]^{2-}$ with CO_2 are consistent with the formation of a CO_2 adduct in which the CO_2 carbon atom binds to the imine carbon atom of the reduced complex and is thus formulated as $[(^i\text{Pr}_2\text{PhPMI})\text{Mo}(\text{CO})_3(\text{CO}_2)]^{2-}$ (Scheme 1).



Scheme 1. Proposed reaction path for the reaction of the dianion $[(^i\text{Pr}_2\text{PhPMI})\text{Mo}(\text{CO})_3]^{2-}$ with CO_2 .

Although unusual, this type of ligand-centered CO_2 binding mode has been observed before. For example, Braunstein et al. in 1981 obtained a similar result to ours by activation of CO_2 at a square planar Pd diphenylphosphinoacetate complex.^[23] Similar binding patterns of carbon dioxide have recently been reported for PNN-Ru^[24] and PNP-Ru/Re^[25] pincer complexes, as well as β -diketiminate $\text{Sc}^{[26]}$ complexes.

Keeping the CO_2 adduct in $[\text{D}_8]\text{THF}$ under an atmosphere of CO_2 causes decomposition with a half-life of about one day. Multiple, so far unidentified products were detected following this process by ^1H NMR spectroscopy. Removal of the solvent and the CO_2 atmosphere, followed by dissolution in fresh $[\text{D}_8]\text{THF}$ enhanced the stability of the CO_2 adduct. This sample showed significantly less decomposition when monitored by ^1H NMR spectroscopy over the course of several days. However, attempts to crystallize or isolate $[(^i\text{Pr}_2\text{PhPMI})\text{Mo}(\text{CO})_3(\text{CO}_2)]^{2-}$ led to decomposition. Crystals that grew from a THF solution at -35°C provided strong evidence for the C–C bond formation between the former imine carbon atom and the CO_2 carbon atom (Figure 6). Only one potassium atom could be located in the Fourier density maps, indicating that the (diamagnetic) CO_2 adduct $[(^i\text{Pr}_2\text{PhPMI})\text{Mo}(\text{CO})_3(\text{CO}_2)]^{2-}$ observed by NMR

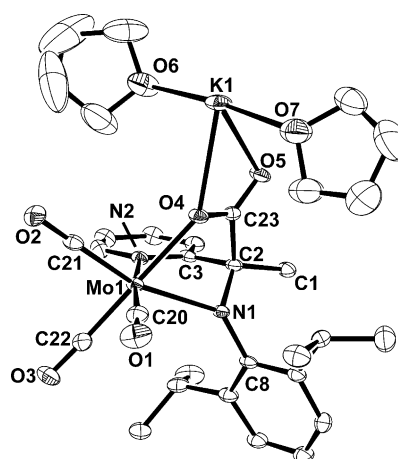


Figure 6. ORTEP representation of the molecular structure of $[(^i\text{Pr}_2\text{PhPMI})\text{Mo}(\text{CO})_3(\text{CO}_2)]\text{K}$, with ellipsoids shown at the 50% probability level. Hydrogen atoms and the co-crystallized, non-coordinated THF molecule are omitted for clarity. Selected bond length (\AA) and angles ($^\circ$): Mo1–N1 2.365(3), Mo1–N2 2.272(3), Mo1–C20 1.948(4), Mo1–C21 1.910(4), Mo1–C22 1.933(4), Mo1–O4 2.283(2), C20–O1 1.173(5), C21–O2 1.181(4), C22–O3 1.178(5), C23–O4 1.273(4), C23–O5 1.230(4), O4–K1 2.834(2), O5–K1 2.748(3), N1–C2 1.527(5), C2–C3 1.523(5), C2–C23 1.572(5); N1–Mo1–C21 164.17(13), N2–Mo1–C20 173.64(13), N1–Mo1–N2 73.76(10), N2–Mo1–C21 101.81(13), N1–Mo1–C20 100.23(14), C20–Mo1–C21 84.54(16), C22–Mo1–O4 175.56(13), N1–Mo1–C22 110.25(12), C21–Mo1–C22 85.17(15), O4–Mo1–C21 96.60(13), N1–Mo1–O4 67.77(9), Mo1–C21–O2 177.5(3), Mo1–C20–O1 176.0(4), Mo1–C22–O3 176.1(3), Mo1–O4–C23 116.9(2), O4–C23–O5 125.8(3), C2–C23–O4 114.8(3), C2–C23–O5 119.4(3), C1–C2–N1 114.4(3), C1–C2–C3 114.0(3), C1–C2–C23 111.3(3), N1–C2–C3 109.3(3), N1–C2–C23 104.1(3), C3–C2–C23 102.5(3), C8–N1–C2 115.3(3), Mo1–N1–C8 137.2(2), Mo1–N1–C2 101.51(19), O4–K1–O5 47.02(7).

spectroscopy either underwent an oxidative process to form a $[(^i\text{Pr}_2\text{PhPMI})\text{Mo}(\text{CO})_3(\text{CO}_2)]^-$ 19 e^- radical monoanion or, more likely, that the charge was compensated by a proton instead of a potassium cation. The most likely protonation site would be the former imine nitrogen atom. Accordingly, refining a hydrogen atom on the former imine nitrogen atom N1 resulted in a stable refinement with almost equal R-values and bonding parameters than without the H atom. Since the presence of a hydrogen atom is not provable by X-ray diffraction alone, the data without the hydrogen atom are presented below and briefly discussed, since the structural data provide additional proof for the C–C coupling that was proposed based on the NMR data.^[27] A comparison of both solutions is provided in the Supporting Information. The central molybdenum ion exhibits a strongly distorted octahedral coordination geometry. Noteworthy is the long Mo1–N1 bond length of 2.365(3) \AA . The molybdenum metal is also bound to one of the former CO_2 oxygen atoms O4. The bond length Mo1–O4 of 2.238(2) \AA is also rather long and consistent with the slow exchange of the three remaining CO ligands observed by ^{13}C NMR spectroscopy. The carbon atom (C23) of the former CO_2 molecule is bound to the former imine carbon atom (C2) of the PMI ligand and a bond length of 1.572(5) \AA is in the order of a C–C single bond.

The CO_2 molecule is bent and, with a sum of angles of 360° , the carbon atom C23 is sp^2 hybridized. Consequentially, the C–O bond lengths C23–O4 (1.273(4) \AA) and C23–O5 (1.230(4) \AA) are consistent with a delocalized C=O double bond and

a small preference for the oxygen atom that is not bound to the molybdenum metal center.^[28] With angles between 102 and 114°, the former imine carbon atom C2 is sp³ hybridized and the N1–C2 (1.527(5) Å) and C2–C3 (1.523(5) Å) bond lengths indicate single bonds.^[28,29] The potassium ion is coordinated by the carboxylate oxygen atom O4 and O5, as well as two THF molecules. The coordination sphere is saturated by two oxygen atoms (O2 and O5) of neighboring molecules (see the Supporting Information, Figure S41).

Despite the incomplete CO₂ reduction in the bulk electrolysis experiment, we investigated the possibility that the carbon atom in the CO₂ adduct could scramble into the carbonyl ligands on the molybdenum ion. However, the ¹³C NMR resonance of free CO is observed at δ = 185 ppm in [D₈]THF^[30] and thus overlaps with the resonance of that in [(^{iPr}₂PhPMI)Mo(CO)₃(CO₂)]²⁻. Nonetheless, no signal enhancement was observed in the resonance at δ = 236 ppm, which is assigned to the carbonyl ligands of [(^{iPr}₂PhPMI)Mo(CO)₃(CO₂)]²⁻ (Figure 5, inset A). The aforementioned formation of side and/or decomposition products indicated by inspection of the ¹H NMR spectrum is confirmed by the ¹³C NMR spectrum of the reaction product(s) in the ¹³CO₂ experiment, where ¹³C incorporation into several products can be observed.

DFT calculations of the reduced complexes

The complex [(^{iPr}₂PhPMI)Mo(CO)₃(CO₂)]²⁻ is not indefinitely stable and attempts to isolate the complex were unsuccessful due to decomposition. Neither were we successful at reliably generating the species in an IR cell in order to corroborate IR data. To gain additional insights into the structure of the CO₂ reduction product, we performed a series of DFT calculations starting with the crystal coordinates of the [(^{iPr}₂PhPMI)Mo(CO)₄] precursor. The bond lengths obtained by DFT are in reasonable agreement with those obtained from the molecular structure (see the Supporting Information, Table S11). The lowest unoccupied molecular orbital (LUMO) of [(^{iPr}₂PhPMI)Mo(CO)₄] is primarily located on the ligand backbone (see the Supporting Information, Figure S43). Not surprisingly, inspection of the highest singly occupied molecular orbital (SOMO) and the Mulliken spin-density surface of the one-electron-reduced species “[(^{iPr}₂PhPMI)Mo(CO)₄]⁻” reveals that the reducing equivalent is predominantly on the ligand and overlays almost identically the LUMO of [(^{iPr}₂PhPMI)Mo(CO)₄] (see the Supporting Information, Figure S44). Earlier we hypothesized, in agreement with the ¹³C NMR and FTIR data, that the second reduction of [(^{iPr}₂PhPMI)Mo(CO)₄] results in loss of a CO ligand and thus optimized the twice reduced species as [(^{iPr}₂PhPMI)Mo(CO)₃]²⁻ (Figure 7 and Figure S45 in the Supporting Information).

Again, inspection of the frontier orbitals reveals predominantly ligand-based reductions. These ligand-based reductions are also evident by a lengthening of the imine C–N bonds from 1.332 Å in the optimized structure of [(^{iPr}₂PhPMI)Mo(CO)₄] to 1.370 Å in [(^{iPr}₂PhPMI)Mo(CO)₄]⁻ and 1.421 Å in [(^{iPr}₂PhPMI)Mo(CO)₃]²⁻. These changes in bond length are accompanied by a contraction of the C–C bond that links the imine carbon to the pyridine moiety, corresponding to greater

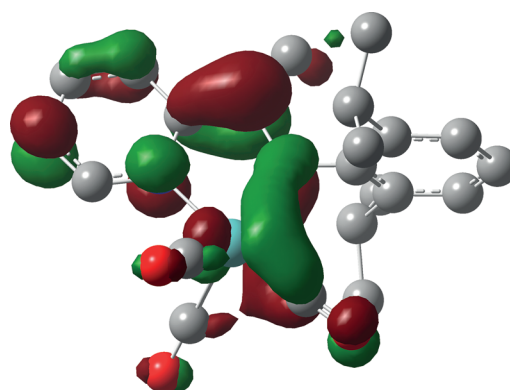


Figure 7. The optimized geometry of [(^{iPr}₂PhPMI)Mo(CO)₃]²⁻ with the overlaid HOMO (iso value = 0.04). Hydrogen atoms have been removed for clarity.

double bond character (1.453 Å to 1.419 Å to 1.392 Å). These changes in bond length upon ligand reduction are well established in the PDI literature. It is less established for pyridine monoketimine complexes, but has been discussed for some pyridine monoaldimine complexes.^[31] We also optimized the CO₂ adduct species with the carbon atom from CO₂ bonded directly to the carbon atom of the imine group (C_{im}; see the Supporting Information, Figure S46). The frontier orbitals of this optimized structure resemble the neutral tetracarbonyl precursor, as opposed to the dianion complex. We take this as support for the hypothesis that the reducing equivalents that ultimately attack CO₂ reside on the ligand, rather than the Mo center. We performed frequency calculations on all four of these geometry-optimized structures to obtain vibrational spectra and compared them to those we obtained in the IR/IR-SEC experiments. The overall patterns for the CO stretching vibrations derived by DFT methods for the tetracarbonyl starting material, as well as the mono- and doubly reduced complexes are in good agreement with the experimentally observed ones (see the Supporting Information, Figures S47–S49). As mentioned earlier, we were unable to reliably prepare IR samples of the CO₂ adduct [(^{iPr}₂PhPMI)Mo(CO)₃(CO₂)]²⁻. However, FTIR spectra in MeCN and THF show close similarities with that derived by DFT methods for the proposed structure (see the Supporting Information, Figures S50 and S51).

Conclusion

In summary we have synthesized and fully characterized two pyridine monoamine (PMI) molybdenum tetracarbonyl complexes, [(^{Ph}PMI)Mo(CO)₄] and [(^{iPr}₂PhPMI)Mo(CO)₄]. These complexes were investigated for electrocatalytic CO₂ reduction and compared to the parent [(bipy)M(CO)₄] system (M = Cr, Mo, W). To gain further insight into the reduction product with CO₂, we used stoichiometric reductant to produce [(^{iPr}₂PhPMI)Mo(CO)₃]²⁻. Subsequent treatment with CO₂ resulted in the formation of a new adduct that displayed cooperative interactions of the metal center and the ligand with CO₂. The NMR spectroscopic investigation provided strong evidence for the proposed structure of [(^{iPr}₂PhPMI)Mo(CO)₃(CO₂)]²⁻, in which the CO₂ carbon atom binds to the imine carbon atom. This structural assign-

ment was further corroborated by DFT calculations. In contrast to other cobalt- or iron-based PDI systems, which appear to be highly covalent, the molybdenum complexes studied herein have a fully separated ligand-based reduction. This manifests in the extremely negative potentials required to access the fully reduced states that react with CO₂. Additionally, the formation of a strong C–C bond between CO₂ and PMI ligand is likely deleterious to catalytic turnover. We are currently investigating the use of the PMI ligands with rhenium and manganese in the hope of driving electrocatalytic CO₂ reduction at more positive potentials.

Acknowledgements

This material is based upon work performed by the Joint Center for Artificial Photosynthesis, a DOE Energy Innovation Hub, supported through the Office of Science of the US Department of Energy under Award Number DE-SC0004993. D.C.L. is supported by the National Institutes of Health (Award Number F32M106726). The authors thank Michael Takase and Lawrence M. Henling for help with the absorption correction of the X-ray data and David VanderVelde for helpful discussions concerning NMR spectroscopy. Jesse D. Froehlich, Charles W. Machan, and Matthew D. Sampson are thanked for the introduction to IR-SEC techniques.

Keywords: CO₂ reduction · electrochemistry · molybdenum · redox-active ligands · spectroelectrochemistry

- a) E. E. Benson, C. P. Kubiak, A. J. Sathrum, J. M. Smieja, *Chem. Soc. Rev.* **2009**, *38*, 89–99; b) B. Kumar, M. Llorente, J. Froehlich, T. Dang, A. Sathrum, C. P. Kubiak, *Annu. Rev. Phys. Chem.* **2012**, *63*, 541–569; c) C. Finn, S. Schnittger, L. J. Yellowlees, J. B. Love, *Chem. Commun.* **2012**, *48*, 1392–1399; d) C. D. Windle, R. N. Perutz, *Coord. Chem. Rev.* **2012**, *256*, 2562–2570; e) C. Costentin, M. Robert, J.-M. Saveant, *Chem. Soc. Rev.* **2013**, *42*, 2423–2436; f) A. M. Appel, J. E. Bercaw, A. B. Bocarsly, H. Dobbek, D. L. DuBois, M. Dupuis, J. G. Ferry, E. Fujita, R. Hille, P. J. A. Kenis, C. A. Kerfeld, R. H. Morris, C. H. F. Peden, A. R. Portis, S. W. Ragsdale, T. B. Rauchfuss, J. N. H. Reek, L. C. Seefeldt, R. K. Thauer, G. L. Waldrop, *Chem. Rev.* **2013**, *113*, 6621–6658.
- J. Hawecker, J.-M. Lehn, R. Ziessel, *J. Chem. Soc. Chem. Commun.* **1984**, 328–330.
- B. P. Sullivan, C. M. Bolinger, D. Conrad, W. J. Vining, T. J. Meyer, *J. Chem. Soc. Chem. Commun.* **1985**, 1414–1416.
- a) P. Christensen, A. Hamnett, A. V. G. Muir, J. A. Timney, *J. Chem. Soc. Dalton Trans.* **1992**, 1455–1463; b) F. P. A. Johnson, M. W. George, F. Hartl, J. J. Turner, *Organometallics* **1996**, *15*, 3374–3387; c) J. M. Smieja, E. E. Benson, B. Kumar, K. A. Grice, C. S. Seu, A. J. M. Miller, J. M. Mayer, C. P. Kubiak, *Proc. Natl. Acad. Sci. USA* **2012**, *109*, 15646–15650; d) K. A. Grice, N. X. Gu, M. D. Sampson, C. P. Kubiak, *Dalton Trans.* **2013**, *42*, 8498–8503; e) E. E. Benson, M. D. Sampson, K. A. Grice, J. M. Smieja, J. D. Froehlich, D. Friebe, J. A. Keith, E. A. Carter, A. Nilsson, C. P. Kubiak, *Angew. Chem. Int. Ed.* **2013**, *52*, 4841–4844; *Angew. Chem.* **2013**, *125*, 4941–4944; f) M. D. Sampson, J. D. Froehlich, J. M. Smieja, E. E. Benson, I. D. Sharp, C. P. Kubiak, *Energy Environ. Sci.* **2013**, *6*, 3748–3755; g) K. A. Grice, C. P. Kubiak in *Advances in Inorganic Chemistry, Vol. 66: CO₂ Chemistry* (Eds.: M. Aresta, R. van Eldik), Academic Press, Waltham, MA, **2014**, pp. 163–188.
- G. J. Stor, F. Hartl, J. W. M. van Outersterp, D. J. Stufkens, *Organometallics* **1995**, *14*, 1115–1131.
- J. M. Smieja, C. P. Kubiak, *Inorg. Chem.* **2010**, *49*, 9283–9289.
- M. D. Sampson, A. D. Nguyen, K. A. Grice, C. E. Moore, A. L. Rheingold, C. P. Kubiak, *J. Am. Chem. Soc.* **2014**, *136*, 5460–5471.
- M. H. B. Stiddard, *J. Chem. Soc.* **1962**, 4712–4715.
- M. L. Clark, K. A. Grice, C. E. Moore, A. L. Rheingold, C. P. Kubiak, *Chem. Sci.* **2014**, *5*, 1894–1900.
- J. Tory, B. Setterfield-Price, R. A. W. Dryfe, F. Hartl, *ChemElectroChem* **2015**, *2*, 213–217.
- R. N. Dominey, B. Hauser, J. Hubbard, J. Dunham, *Inorg. Chem.* **1991**, *30*, 4754–4758.
- D. C. Lacy, C. C. L. McCrory, J. C. Peters, *Inorg. Chem.* **2014**, *53*, 4980–4988.
- S. S. Braga, A. C. Coelho, I. S. Goncalves, F. A. Almeida Paz, *Acta Crystallogr. Sect. E* **2007**, *63*, m780–m782.
- a) B. de Bruin, E. Bill, E. Bothe, T. Weyhermüller, K. Wieghardt, *Inorg. Chem.* **2000**, *39*, 2936–2947; b) P. H. M. Budzelaar, B. de Bruin, A. W. Gal, K. Wieghardt, J. H. van Lenthe, *Inorg. Chem.* **2001**, *40*, 4649–4655; c) Q. Knijnenburg, S. Gambarotta, P. H. M. Budzelaar, *Dalton Trans.* **2006**, 5442–5448.
- K. Nienkemper, V. V. Kotov, G. Kehr, G. Erker, R. Fröhlich, *Eur. J. Inorg. Chem.* **2006**, 366–379.
- J. Lewis, M. Schroder, *J. Chem. Soc. Dalton Trans.* **1982**, 1085–1089.
- a) S. P. Best, R. J. H. Clark, R. C. S. McQueen, R. P. Cooney, *Rev. Sci. Instrum.* **1987**, *58*, 2071–2074; b) K. Ashley, S. Pons, *Chem. Rev.* **1988**, *88*, 673–695; c) J. P. Bullock, K. R. Mann, *Inorg. Chem.* **1989**, *28*, 4006–4011; d) C. W. Machan, M. D. Sampson, S. A. Chabolla, T. Dang, C. P. Kubiak, *Organometallics* **2014**, *33*, 4550–4559.
- The orange solution also formed when a sodium metal or Na/Hg was used as the reductant. NMR spectroscopic investigation indicated a paramagnetic product, which is therefore assigned to the putative monoanion [^{(*η*-Ph)PMI)Mo(CO)₄]⁻, which was not further investigated in this study.}
- D. Sieh, M. Schlimm, L. Andernach, F. Angersbach, S. Nüchel, J. Schöffel, N. Šušnjar, P. Burger, *Eur. J. Inorg. Chem.* **2012**, 444–462.
- Leibfritz, H. tom Dieck, *J. Organomet. Chem.* **1976**, *105*, 255–261.
- a) L. J. Todd, J. R. Wilkinson, J. P. Hickey, D. L. Beach, K. W. Barnett, *J. Organomet. Chem.* **1978**, *154*, 151–157; b) P. C. Lauterbur, R. B. King, *J. Am. Chem. Soc.* **1965**, *87*, 3266–3267.
- H.-O. Kalinoswki, S. Berger, S. Braun, *Carbon-13 NMR Spectroscopy*, John Wiley & Sons, Ltd., Chichester, UK, **1988**.
- P. Braunstein, D. Matt, Y. Dusaouy, J. Fischer, A. Mitschler, L. Ricard, *J. Am. Chem. Soc.* **1981**, *103*, 5115–5125.
- C. A. Huff, J. W. Kampf, M. S. Sanford, *Organometallics* **2012**, *31*, 4643–4645.
- a) M. Vogt, M. Gargir, M. A. Iron, Y. Diskin-Posner, Y. Ben-David, D. Milstein, *Chem. Eur. J.* **2012**, *18*, 9194–9197; b) M. Vogt, A. Nerush, Y. Diskin-Posner, Y. Ben-David, D. Milstein, *Chem. Sci.* **2014**, *5*, 2043–2051; c) G. A. Filonenko, M. P. Conley, C. Copéret, M. Lutz, E. J. M. Hensen, E. A. Pidko, *ACS Catal.* **2013**, *3*, 2522–2526.
- F. A. LeBlanc, A. Berkefeld, W. E. Piers, M. Parvez, *Organometallics* **2012**, *31*, 810–818.
- A protonation of the imine nitrogen atom is, however, supported by resonances at 6.03 and 5.50 ppm, that could be detected in the ¹H NMR spectrum crystalline material (see the Supporting Information, Figure S37).
- F. H. Allen, O. Kennard, D. G. Watson, L. Brammer, A. G. Orpen, R. Taylor, *J. Chem. Soc. Perkin Trans. 2* **1987**, S1–S19.
- Note that the rather long C–N bond length of 1.527(5) Å might also be indicative of a protonated nitrogen atom.
- a) D. Sellmann, R. Prakash, F. W. Heinemann, *Eur. J. Inorg. Chem.* **2004**, 1847–1858; b) C. Blanco, C. Godard, E. Zangrando, A. Ruiz, C. Claver, *Dalton Trans.* **2012**, *41*, 6980–6991.
- a) C. C. Lu, E. Bill, T. Weyhermüller, E. Bothe, K. Wieghardt, *J. Am. Chem. Soc.* **2008**, *130*, 3181–3197; b) C. C. Lu, T. Weyhermüller, E. Bill, K. Wieghardt, *Inorg. Chem.* **2009**, *48*, 6055–6064; c) M. van Gastel, C. C. Lu, K. Wieghardt, W. Lubitz, *Inorg. Chem.* **2009**, *48*, 2626–2632; d) T. W. Myers, N. Kazem, S. Stoll, R. D. Britt, M. Shanmugam, L. A. Berben, *J. Am. Chem. Soc.* **2011**, *133*, 8662–8672; e) T. W. Myers, G. M. Yee, L. A. Berben, *Eur. J. Inorg. Chem.* **2013**, 3831–3835.

Received: February 4, 2015

Published online on April 29, 2015